International Journal of Mechanics and Energy (IJME)
Vol. 2, Issue 1, 2014, ISSN: 2286-5845

Effect of Thermal Rayleigh Number and Buoyancy Ratio on the Fluid Flow, Heat and Mass Transfer in a Salt–Gradient Pond

Ridha Boudhiaf *, Mounir Baccar

Computational Fluid Dynamics and Transfer Phenomena (CFDTP), National School of Engineers of Sfax (ENIS), University of Sfax (US), B.P. 1173, Road Soukra km 3.5, 3038 Sfax, TUNISIA

Mobile: (+216) 99 812 853; Tel.: (+216) 74 274 409/418 (ext. 395); fax: (+216) 74 275 595

Abstract: In this paper, we studied numerically the effect of thermal Rayleigh number and the buoyancy ratio on the transient fluid flow, heat and mass transfer in a salt–gradient pond (SGP) wherein the layers of fluid are stratified. The objective of this numerical work is to give a fine knowledge of the hydrodynamic, thermal and solute characteristics during the storage of thermal energy in a SGP. The pond is filled with a mixture of salt and water to constitute three zones with different salinities: Upper Convective Zone (UCZ), Non–Convective Zone (NCZ) and Lower Convective Zone (LCZ). Water is heated by a heat serpentine covered the bottom of the pond. The transport equations for continuity, momentum, thermal energy and mass transfer are solved by a finite–volume method to provide the fields of temperature, concentration and velocities in a SGP in transient regime. Simulations are performed for several values of both the thermal Rayleigh number in the range between 10^4 and 10^7, and the buoyancy ratio in the range between 0 and 10, whose influence on the temporal evolution of velocities, temperature and concentration distributions in a SGP are analyzed and discussed. The flow structure shows the generation of convective cells in the lower and upper zones of the pond, and permits to explain the slight increase of temperature in the UCZ and the important rise of temperature in the LCZ. In addition, this work shows the importance of the buoyancy ratio to preserve the high temperature in the bottom of the pond and to reduce the phenomena of heat and mass transfer across the NCZ.

Key words: Stratified fluid layers; Salt–gradient pond; Hydrodynamic, heat and mass transfer; Numerical simulation; Finite–volume method; Transient regime.

1. Introduction

Salt–gradient pond is a large pool that stores a great amount of thermal energy for a long period of time throughout months, seasons or even a year.

Thermal energy stored is used in several applications that include heating of buildings, production of electricity, heat-pumps, boilers, and textile processing and food industries. The pond is made up of a rectangular cavity filled with a mixture of salt and water and subdivided into three distinct zones characterized by different salinities. The first zone is called the upper convective zone "UCZ" which is cold and close to the ambient temperature. It has a low salt concentration. The second convective zone is situated at the bottom and called lower convective zone "LCZ" characterized by a high temperature between 70 and 100°C, and a maximum salt concentration. These two zones are characterized by nearly homogeneous concentration and separated by the important gradient zone called non–convective zone "NCZ", where salt content increases with depth. At the level of this zone, water cannot ascend for two reasons: Firstly, the light quantity of salt contained in the upper water makes it lighter than the lower water, and the second reason is that the lower water contains greater amount of salt making it in turn heavier. The NCZ acts as a transparent insulator.

Many studies have been done on salt–gradient ponds. Tabor [1] and Shahar [2] presented an experimental setup of salt–gradient pond. Bryant et al. [3], Hawlader [4], Newell et al. [5] and Alagao et al.

*** Corresponding author:** Ridha Boudhiaf
E-mail: ridhaboudhiaf@yahoo.fr

[6] concentrated their effort to study the thermal performances of various types of different dimensions salt–gradient ponds. Srinivasan and Guha [7] considered two phases of thermal behaviour of salt–gradient pond. In the first one, a linear temperature profile in the NCZ and a constant temperature in the UCZ and in the LCZ are imposed. In the second phase, the temperature of the LCZ oscillates as a function of the fluctuation of the received net solar radiation energy, which is particularly related to the season of the year. Jamal and Khashan [8] developed a mathematical model to determine the different parameters affecting the salt–gradient pond performance. They showed that the thickness of NCZ has an important effect on the storage of thermal energy. The study of Huseyin et al. [9] showed that the salt–gradient pond can store thermal energy for a long period of time. The research of Huanmin et al. [10] showed that the storage of thermal energy allows salt–gradient pond to power desalination during cloudy days and night time. Kumar and Kishore [11] showed that salt–gradient pond has recently become an important source of thermal energy which is used in several applications such as desalination of sea–water and electricity production. Recently, Hammami et al. [12] studied numerically the transient hydrodynamic and thermal behavior in a salt–gradient pond. This research is limited to thermal Rayleigh number equal to 5 10^4 and neglected the effect of buoyancy ratio on the stability of the SGP. The authors showed the presence of recirculation zones caused only in the LCZ.

In this research work, we present a two–dimensional numerical study of the effect of thermal Rayleigh number and buoyancy ratio on the fluid flow, heat and mass transfer in a salt–gradient pond and its stability during the storage of thermal energy. The bottom of the pond is heated uniformly by a heat serpentine and the free surface is cooled at ambient temperature while the two vertical walls are adiabatic and impermeable. The pond that contains a mixture of salt and water is constituted by three different salinity zones. Our objective is to give a better understanding of the transient evolution of temperature, concentration and velocities fields developed in a salt–gradient pond.

2. Mathematical Formulation

2.1 Governing Equations

The geometry investigated is a pond filled with a mixture of water and salt, and is modeled by a rectangular cavity of height H and length L. The vertical walls of the pond are adiabatic and impermeable. The bottom and the free surface are also impermeable. The fluid is heated at constant hot temperature (T_h) by a heat serpentine covering the entire of the bottom of the pond. The free surface of the pond is cooled at ambient temperature (T_a). In this study, the solar radiation absorption is not considered into account, so we consider a storage application. The geometry and dimensionless coordinate system are shown in Figure 1.

The fluid is assumed to be Newtonian and incompressible, with constant thermo–physical properties. In the buoyancy term, the density is taken as a function of both the local temperature and concentration through the approximation of Boussinesq,

$$\rho(T,C) = \rho_0\left(1-\beta_T\left(T-T_a\right)+\beta_S\left(C-C_{min}\right)\right) \qquad (1)$$

where $\beta_T = -1/\rho_0(\partial\rho/\partial T)_C$ and $\beta_S = -1/\rho_0(\partial\rho/\partial C)_T$.

The height of the pond (H) is taken as a scale length for the spatial coordinates (X = x/H and Z = z/H). Time, velocity, pressure, temperature and concentration scales are defined as: H^2/α, α/H, $\rho\alpha^2/H^2$, $\Delta T=T_h-T_a$ and $\Delta C=C_{max}-C_{min}$, respectively.

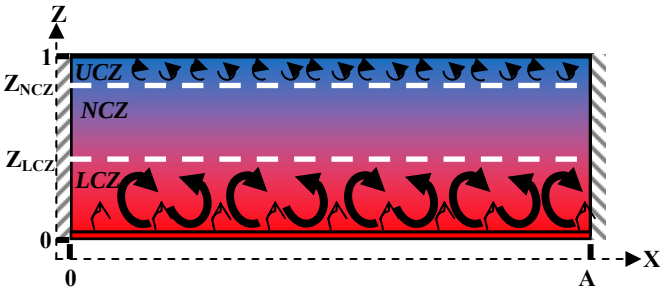

Fig. 1. Geometry of the studied salt–gradient pond.

The dimensionless equations of continuity, momentum, thermal energy and mass transfer can be written as follow:

$$\mathrm{div}\vec{V}=0 \tag{2}$$

$$\frac{\partial U}{\partial \tau}+\mathrm{div}\left(U\vec{V}-\mathrm{Pr}\ \overrightarrow{\mathrm{grad}}\,U\right)=-\frac{\partial P}{\partial X} \tag{3}$$

$$\frac{\partial W}{\partial \tau}+\mathrm{div}\left(W\vec{V}-\mathrm{Pr}\ \overrightarrow{\mathrm{grad}}\,W\right)=-\frac{\partial P}{\partial Z}+\mathrm{Pr}\,\mathrm{Ra}_T\left(\theta-N\varphi\right) \tag{4}$$

$$\frac{\partial \theta}{\partial \tau}+\mathrm{div}\left(\theta\vec{V}-\overrightarrow{\mathrm{grad}}\,\theta\right)=0 \tag{5}$$

$$\frac{\partial \varphi}{\partial \tau}+\mathrm{div}\left(\varphi\,\vec{V}-\frac{1}{\mathrm{Le}}\overrightarrow{\mathrm{grad}}\,\varphi\right)=0 \tag{6}$$

The above equations have been made dimensionless using the following variables:

$X = x/H$, $Z = z/H$, $U = u\,H/\alpha$, $W = w\,H/\alpha$, $\theta = (T-T_a)/\Delta T$, $\varphi = (C-C_{min})/\Delta C$, $P = pH^2/(\rho_0\alpha^2)$, $\tau = \alpha\,t/H^2$ (7)

The dimensionless parameters that characterize the salt–gradient pond are the aspect ratio A=L/H, the thermal Rayleigh number $Ra_T = (g\,\beta_T\,\Delta T\,H^3)/\alpha\nu$, the solutal Rayleigh number $Ra_S = (g\,\beta_S\,\Delta C\,H^3)/\alpha\nu$, the buoyancy ratio $N = \beta_S\Delta C/\beta_T\Delta T$, the Prandtl number $Pr = \nu/\alpha$, the Schmidt number $Sc = \nu/D$ and the Lewis number $Le = Sc/Pr$.

2.2 Boundary and Initial Conditions

Initially, the fluid is supposed to be at a stagnation state (U = W = 0 and P = 0) and has an ambient temperature (θ = 0). The initial dimensionless salt concentration is disturbed in the pond as follows:

$0 \le Z \le Z_{LCZ}$, $\varphi = 1$ (8a)

$Z_{LCZ} \le Z \le Z_{NCZ}$, $\varphi = (Z_{NCZ}-Z)/(Z_{NCZ}-Z_{LCZ})$ (8b)

$Z_{NCZ} \le Z \le Z_{UCZ}$, $\varphi = 0$ (8c)

The dimensionless thicknesses of LCZ and NCZ, $E_{LCZ} = E_{NCZ} = 0.4$ and that of UCZ, $E_{UCZ} = 0.2$ (Boudhiaf et al. [13]).

The boundary conditions are the non–slip condition at the vertical walls and the bottom of the pond (U=W=0). The constant temperatures are adopted along the bottom and the free surface, and adiabatic and impermeable conditions on the vertical walls. Hence,

$\partial\theta/\partial X = 0$ and $\partial\varphi/\partial X = 0$ at $X = 0$ (9a)

$\theta = 1$ and $\partial\varphi/\partial Z = 0$ at $Z = 0$ (9b)

$\theta = 0$, $\partial\varphi/\partial Z = 0$, $\partial U/\partial Z = 0$ and $W = 0$ at $Z = 1$ (9c)

For reasons of symmetry, we consider only half of the pond. Therefore, the boundaries U=0, $\partial W/\partial X = 0$, $\partial\theta/\partial X = 0$ and $\partial\varphi/\partial X = 0$ are taken in the symmetrical vertical plane (X=A/2).

3. Numerical Method

Finite–volume method developed by Patankar [14] is employed to discretize the equations (2–6) on a staggered grid. A hybrid scheme is adopted for the convection–diffusion formulation. The discretized equations obtained are solved over a time step, using the Alterning Directions Implicit (ADI) method. Pressure–velocity coupling is handled by using the Semi–Implicit Method for Pressure–Linked Equation Revised (SIMPLER) algorithm described in details by Patankar [14].

The numerical method and the validation of the numerical code specifically developed for the present study have been described in details by Boudhiaf et al. [13].

A computational domain consisting of 50x100 grid points with uniform grid spacing in OX and in OZ, and a dimensionless time step equal to 10^{-8} were found to

be sufficient for producing accurate results at reasonable computing time.

4. Results and discussion

In this work, we present a numerical study in transient regime to better understand the temporal evolution of the hydrodynamic, heat and mass transfer structures induced in a salt–gradient pond of an aspect ratio equal to three. The particular interest of this numerical study is to control the fluid flow, heat and mass transfer parameters for double–diffusive natural convection in the pond. These parameters are aspect ratio, thermal Rayleigh number between 10^4 and 10^7, Prandtl number, buoyancy ratio and Schmidt number. The range of Ra_T covers most of the engineering applications. The numerical results are given for constant values of the Prandtl number Pr = 6 and the Schmidt number Sc = 1000, which correspond to the averaged characteristics of salt–water mixture (Hammami et al. [12] ; Boudhiaf et al. [13]).

4.1 Effect of the thermal Rayleigh number

The effect of thermal Rayleigh number on the transient evolution of temperature, concentration and velocities fields is represented in Figs. 2-7 for Pr = 6, Sc = 1000, N = 10 and A = 3. Fig. 2 shows that for thermal Rayleigh number equal to 10^4, the heat transfer is oriented in the vertical direction by diffusion.

If the thermal Rayleigh number is increased to 10^5, Fig. 3 shows that the heat transfer by convection becomes dominating and the temperature gradient starts to increase with time in the LCZ.

At thermal Rayleigh number equal to 10^6, Fig. 4 shows that the convective heat transfer is more pronounced. At τ = 0.0035, the liquid warms and develops a two-cell thermal pattern which are symmetrical in the lower corners of the pond's bottom. When the time increases, the number of cells starts to increase in the LCZ.

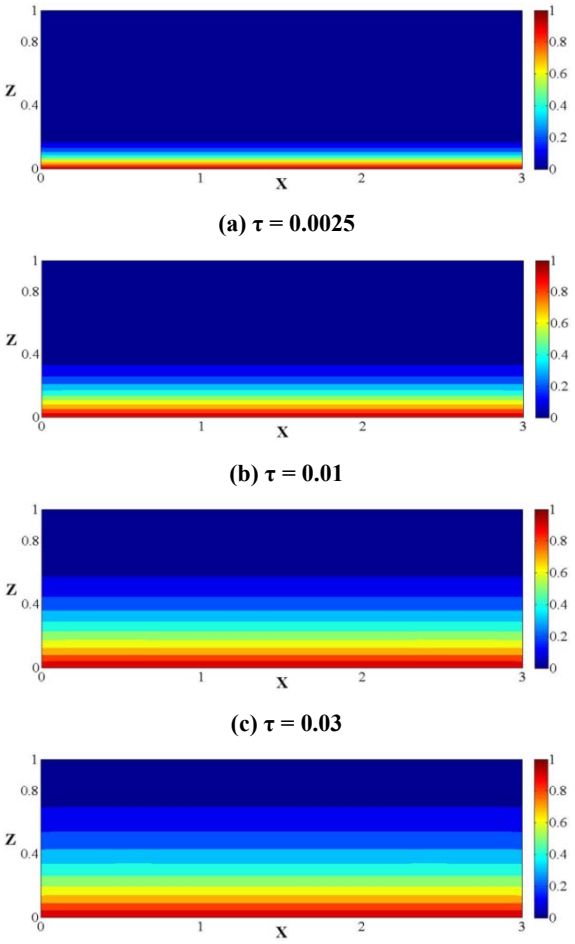

(a) τ = 0.0025

(b) τ = 0.01

(c) τ = 0.03

(d) τ = 0.045

Fig. 2. Transient evolution of temperature field in a salt–gradient pond.
($Ra_T = 10^4$, Pr = 6, Sc = 1000, N = 10 and A = 3)

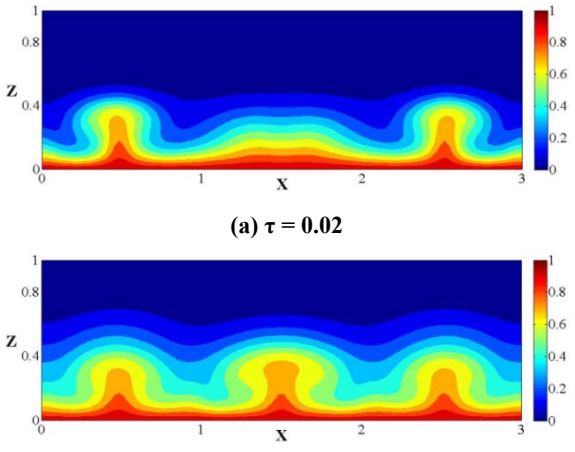

(a) τ = 0.02

(b) τ = 0.03

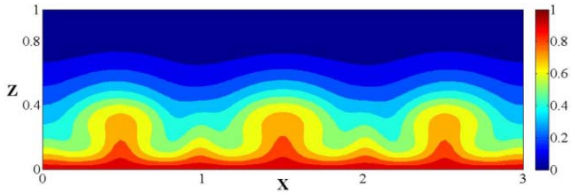

(c) τ = 0.035

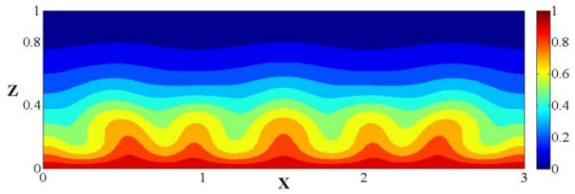

(d) τ = 0.045

Fig. 3. Transient evolution of temperature field in a salt–gradient pond.
($Ra_T = 10^5$, Pr = 6, Sc = 1000, N = 10 and A = 3)

Fig. 5 shows that the temperature gradient increases with time and the number of large thermal cells with uniform temperature starts to increase in the LCZ. Small thermal cells begin to be formed in the UCZ (Fig. 5c). These thermal cells are more developed in the UCZ (Fig. 5d).

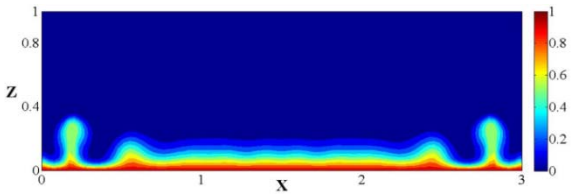

(a) τ = 0.0035

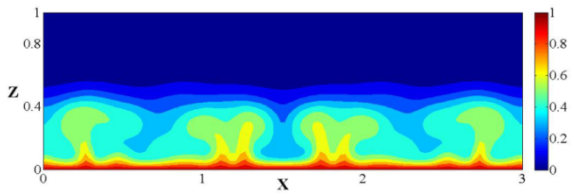

(b) τ = 0.01

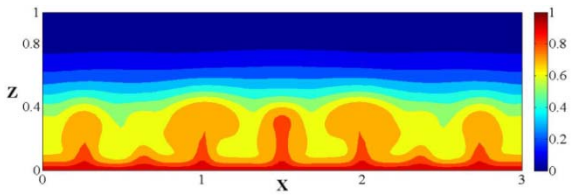

(c) τ = 0.025

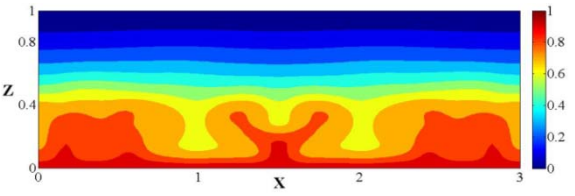

(d) τ = 0.045

Fig. 4. Transient evolution of temperature field in a salt–gradient pond.
($Ra_T = 10^6$, Pr = 6, Sc = 1000, N = 10 and A = 3)

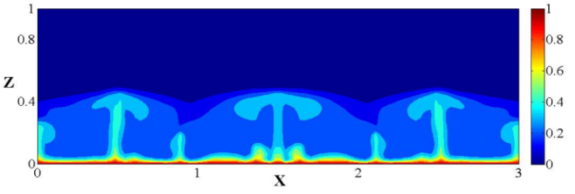

(a) τ = 0.0025

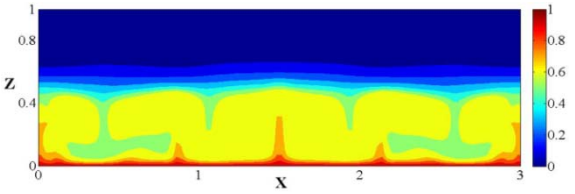

(b) τ = 0.01

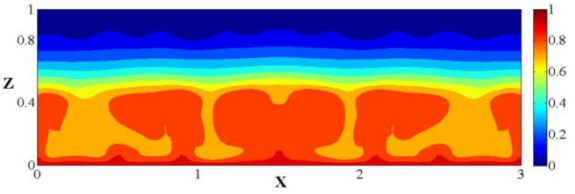

(c) τ = 0.025

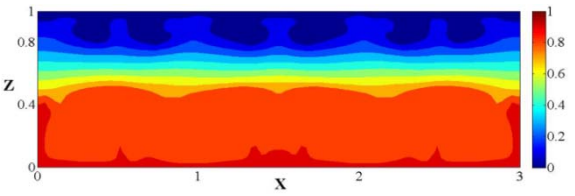

(d) τ = 0.045

Fig. 5. Transient evolution of temperature field in a salt–gradient pond.
($Ra_T = 10^7$, Pr = 6, Sc = 1000, N = 10 and A = 3)

Thermal and hydrodynamic behaviors are coupled in natural convective regime. Therefore, to better

understand the distribution of temperature, we have reproduced in Fig. 6, the evolution of velocities distribution with Ra_T.

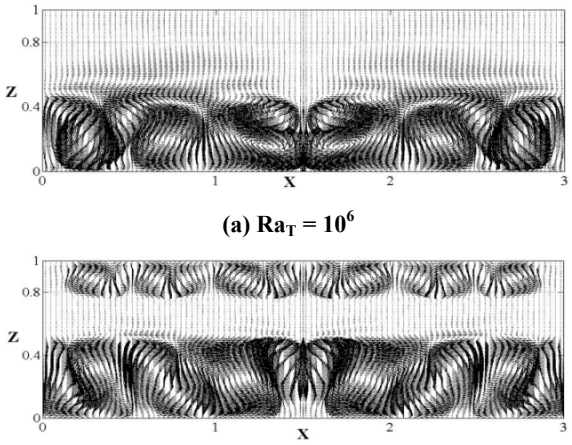

(a) $Ra_T = 10^6$

(b) $Ra_T = 10^7$

Fig. 6. Effect of Ra_T on the distribution of velocities in a salt–gradient pond at $\tau = 0.045$. (Pr = 6, Sc = 1000, N = 10 and A = 3)

It may be seen from Fig. 6(a) the presence of multi–cells of the flow field localized only in the lower convective zone of the pond. At thermal Rayleigh number $Ra_T = 10^7$ (Fig. 6(b)), a succession of symmetrical cells flow pattern is generated in the UCZ and in the LCZ. These cells of the flow field contribute to the homogenization of the LCZ and enhance the temperature gradient from the bottom of the pond. In this case, the stagnation fluid motion is observed in the NCZ.

The evolution of concentration field with thermal Rayleigh number is presented in Fig. 7 at $\tau = 0.045$ and for $Ra_T = 10^6$-10^7, Pr = 6, Sc = 1000, N = 10 and A = 3. It may be noticed from Fig. 7 that the salty water layers in the pond remain stable when the thermal Rayleigh number increases from 10^6 to 10^7. This figure shows also that the increase of thermal Rayleigh number will decrease the thickness of NCZ.

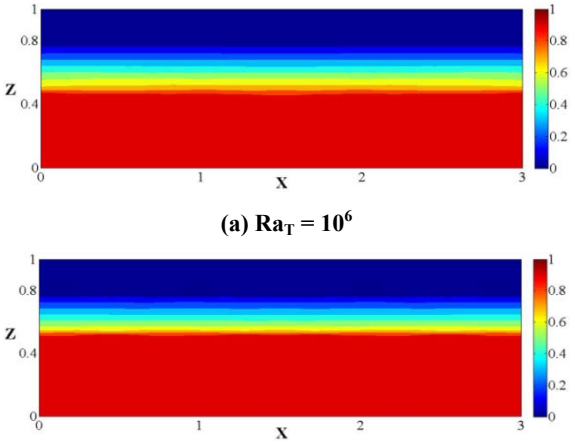

(a) $Ra_T = 10^6$

(b) $Ra_T = 10^7$

Fig. 7. Effect of Ra_T on the concentration distribution in a salt–gradient pond at $\tau = 0.045$. (Pr = 6, Sc = 1000, N = 10 and A = 3)

4.2 Effect of buoyancy ratio

The effect of buoyancy ratio on the temperature, velocities and concentration distributions for $Ra_T = 10^7$, Pr = 6, Sc = 1000 and A = 3 is shown in Figs. 8-16. Figs. 8 and 9 show the transient evolution of temperature and velocities distributions in a convective pond for N = 0.

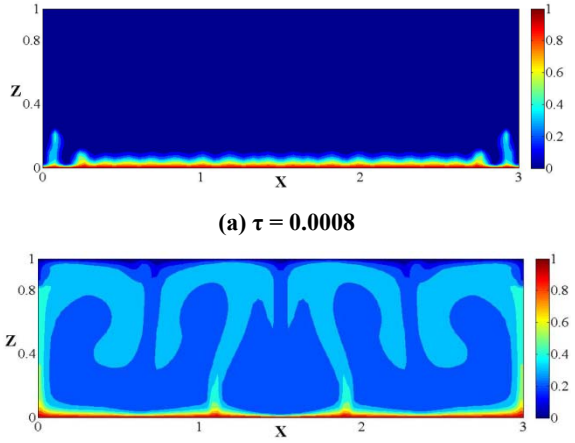

(a) $\tau = 0.0008$

(b) $\tau = 0.008$

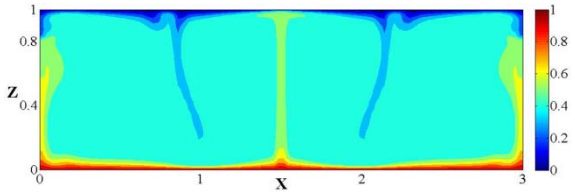

(c) τ = 0.025

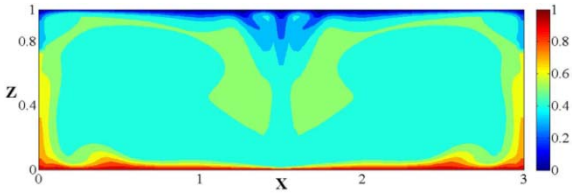

(d) τ = 0.045

Fig. 8. Transient evolution of temperature distribution in a convective pond.

($Ra_T = 10^7$, N = 0, Pr = 6, Sc = 1000 and A = 3)

Fig. 8 shows that for a buoyancy ratio equal to zero (without salt gradient), the convective motions prevent the storage of thermal energy in the bottom of the pond. Because the warmer fluid is lighter, it rises to the free surface and loses a part of its heat to the ambient air. At the free surface of the pond, the cold fluid is heavier, and so it sinks to the bottom of the pond. In this case, the convective circulation occurring in the fluid is due to the effect of thermal buoyancy force. This important convective circulation and the heat loss through the free surface prevent the storage of thermal energy in the convective pond.

Fig. 9(a) shows two little recirculations in the lower corners of the pond. Then, these recirculations are developed with time and occupy the entire of the convective pond (Fig. 9(b)).

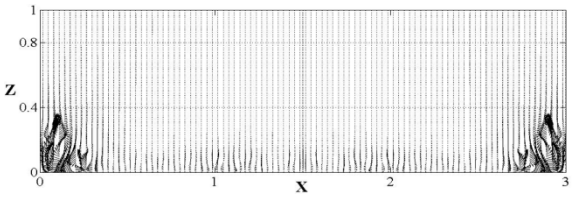

(a) τ = 0.0008

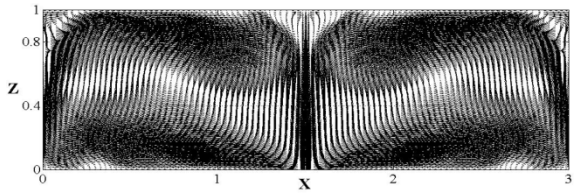

(b) τ = 0.045

Fig. 9. Transient evolution of velocities distribution in a convective pond.

($Ra_T = 10^7$, N = 0, Pr = 6, Sc = 1000 and A = 3)

Figs. 10, 11 and 12 show the transient evolution of temperature distribution in a salt–gradient pond for N = 2, 4 and 10, respectively.

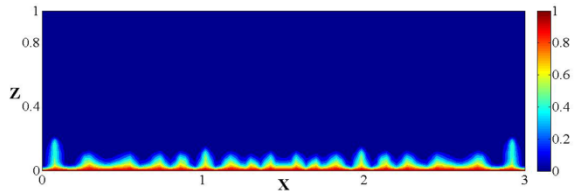

(a) τ = 0.0008

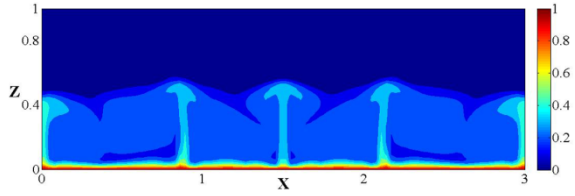

(b) τ = 0.0025

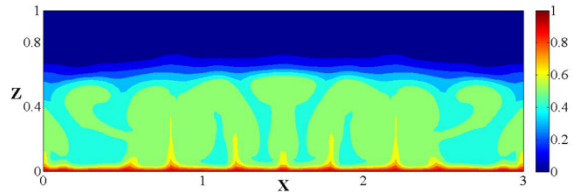

(c) τ = 0.008

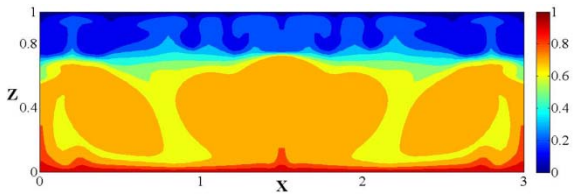

(d) τ = 0.025

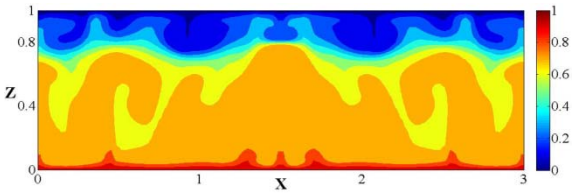

(e) τ = 0.045

Fig. 10. Transient evolution of temperature distribution in a salt–gradient pond.
($Ra_T = 10^7$, N = 2, Pr = 6, Sc = 1000 and A = 3)

For a buoyancy ratio equal to 2 (Fig. 10), the upward heat losses increase with time and the storage of thermal energy destroys.

In Fig. 11, we can observe an increase, with time, of temperature in the UCZ and in the LCZ. In Fig. 11(e), a thin non–convective zone begins to be formed.

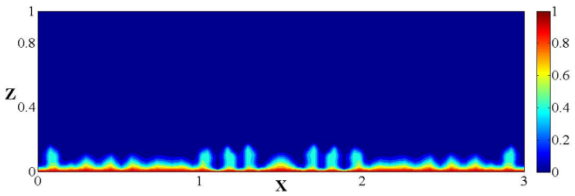

(a) τ = 0.0008

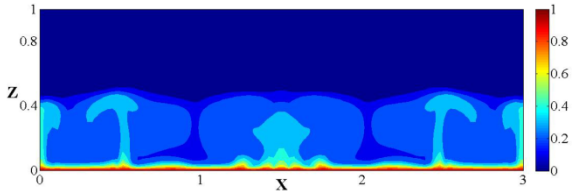

(b) τ = 0.0025

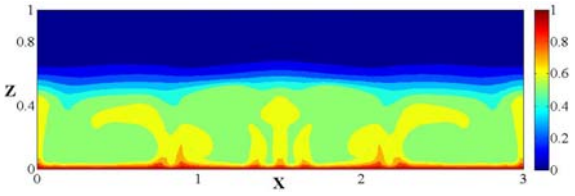

(c) τ = 0.0085

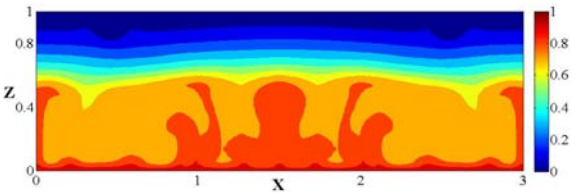

(d) τ = 0.0254

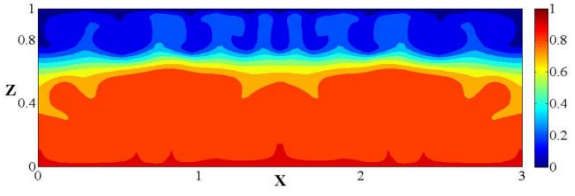

(e) τ = 0.045

Fig. 11. Transient evolution of temperature distribution in a salt–gradient pond.
($Ra_T = 10^7$, N = 4, Pr = 6, Sc = 1000 and A = 3)

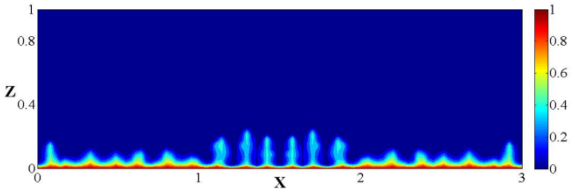

(a) τ = 0.0008

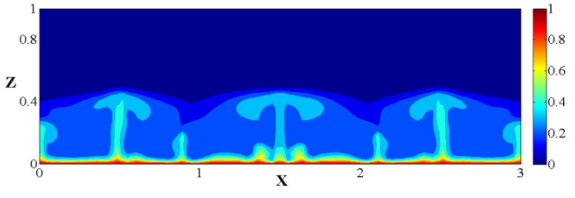

(b) τ = 0.0025

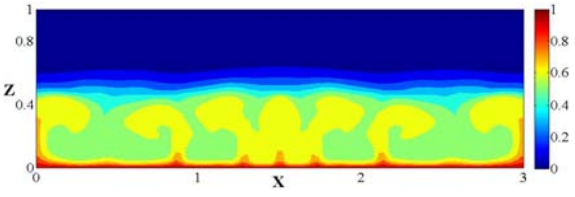

(c) τ = 0.0085

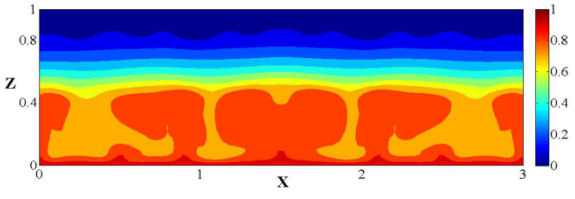

(d) τ = 0.025

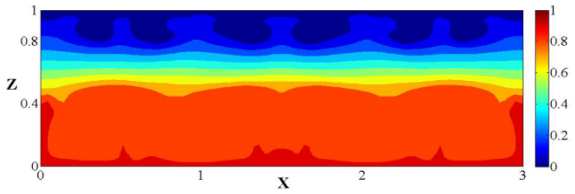

(e) τ = 0.045

Fig. 12. Transient evolution of temperature distribution in a salt–gradient pond.
($Ra_T = 10^7$, N = 10, Pr = 6, Sc = 1000 and A = 3)

At τ = 0.0008 (Fig. 12(a)), the salty water warms up and develops thermal gradient in the pond's bottom which results a growing up of multi-cellular thermal patterns (Fig. 12(b)-(c)). Fig. 12(d) shows the presence of corrugations at the NCZ-UCZ interface and a rise of temperature in the LCZ. Then, the temperature increases with time and thermal cells tend to be collapsed to form a uniform temperature in the LCZ (Fig. 12(e)). In this figure, we can see also a succession of thin thermal cells generated in the UCZ. Hence, the salt gradient has a considerable role to maintain high temperature in the LCZ and to reduce the heat losses across the NCZ of the pond.

To better understand the effect of buoyancy ratio on the thermal behavior of SGP, we have reproduced in Fig. 13 the evolution of velocities distribution with buoyancy ratio in a salt–gradient pond at τ = 0.045. In Fig. 13(a), we observe a single convection zone in the pond due to the suppression of the NCZ and the increase in the size of the upper and lower convective zones.

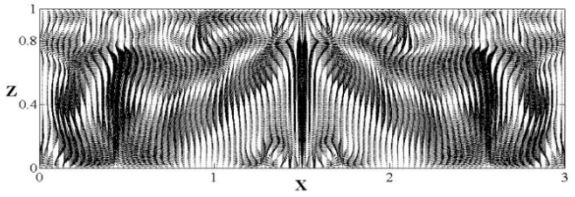

(a) N = 2

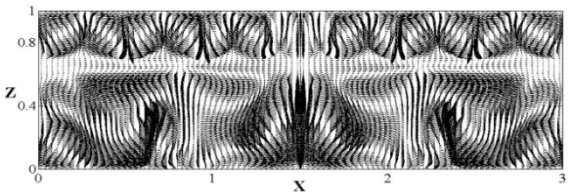

(b) N = 4

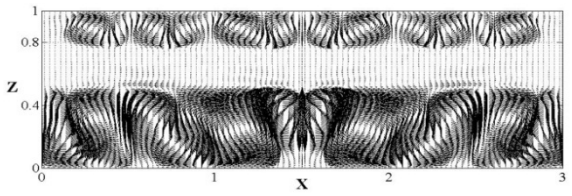

(c) N = 10

Fig. 13. Effect of buoyancy ratio on the velocities distribution in a salt–gradient pond at τ = 0.045.
($Ra_T = 10^7$, Pr = 6, Sc = 1000 and A = 3)

Fig. 13(b) shows the appearance of thin NCZ. For a buoyancy ratio equal to 10 (Fig. 13(c)), we observe the presence of three zones in the SGP: the upper convective zone (UCZ) with many small eddies, the non–convective zone (NCZ) wherein the fluid is stagnant and the lower convective zone (LCZ) with many large recirculations.

For a buoyancy ratio equal to 2 (Fig. 14), the NCZ is suppressed with time due to the diffusion of salt from LCZ to UCZ. In this case, the size of LCZ and UCZ increases with time to give a homogeneous pond.

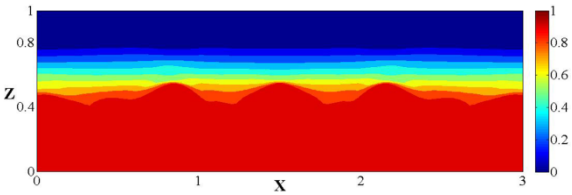

(a) τ = 0.0025

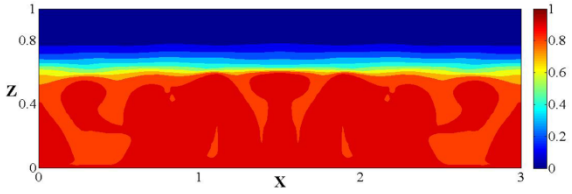

(b) τ = 0.008

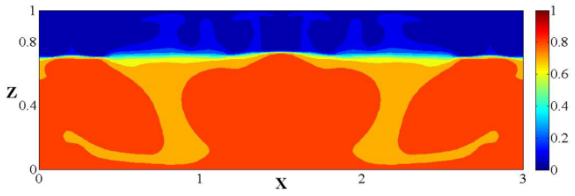

(c) τ = 0.025

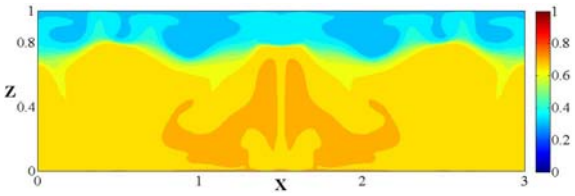

(d) τ = 0.045

Fig. 14. Transient evolution of concentration distribution in a salt–gradient pond.
($Ra_T = 10^7$, Pr = 6, Sc = 1000, N = 2 and A = 3)

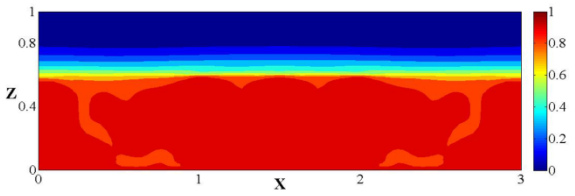

(c) τ = 0.025

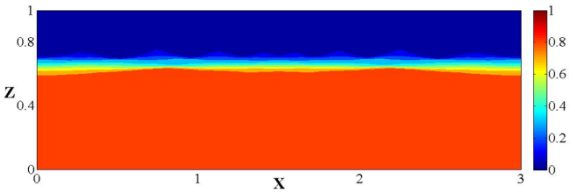

(d) τ = 0.045

Fig. 15. Transient evolution of concentration distribution in a salt–gradient pond.
($Ra_T = 10^7$, Pr = 6, Sc = 1000, N = 4 and A = 3)

Fig. 15 shows that the thickness of NCZ decreases with time. When the buoyancy ratio increases to 10 (Fig. 16), we observe a slight diffusion of salt with time from the bottom to the free surface of the pond due to the rise of temperature in the LCZ. Fig. 16 shows also that the thickness of NCZ decreases slightly with time and the stratified fluid layers are stable in the salt–gradient pond.

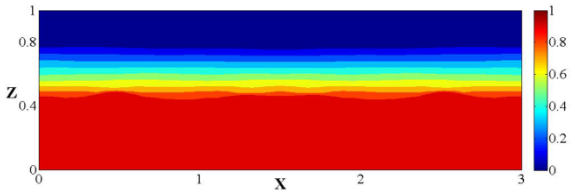

(a) τ = 0.0025

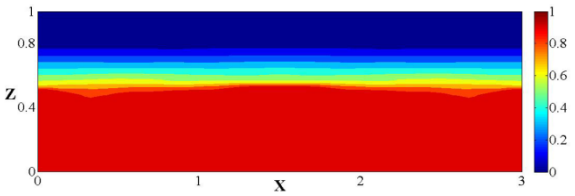

(b) τ = 0.008

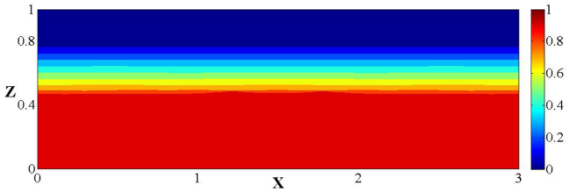

(a) τ = 0.008

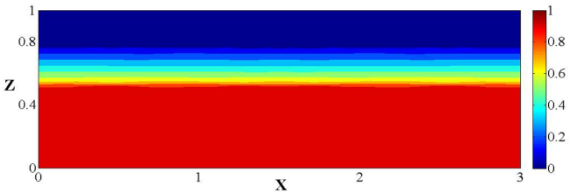

(b) τ = 0.045

Fig. 16. Transient evolution of concentration distribution in a salt–gradient pond.
($Ra_T = 10^7$, Pr = 6, Sc = 1000, N = 10 and A = 3)

4.3 Development of the average temperature and concentration profiles

The effect of thermal Rayleigh number on the development of the average temperature profile in a salt–gradient pond for N = 10 and A = 3 at τ = 0.045 is shown in Fig. 17.

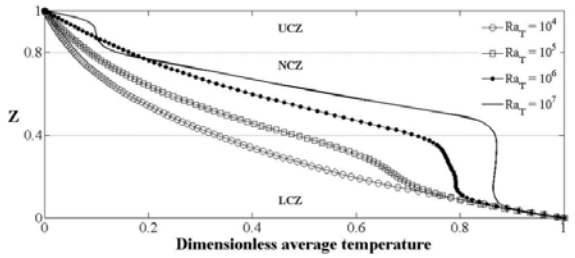

Fig. 17. Effect of Ra_T on the average temperature profile in a salt–gradient pond at $\tau = 0.045$. (N = 10, Pr = 6, Sc = 1000 and A = 3)

Fig. 17 shows that the increase of thermal Rayleigh number will increase the average temperature profile in the three zones constituting the pond. In the vicinity of the pond's bottom, the four profiles of average temperature are confused.

The effect of buoyancy ratio on the development of the average temperature profile in a salt–gradient pond for $Ra_T = 10^7$ and A = 3 at $\tau = 0.045$ is shown in Fig. 18.

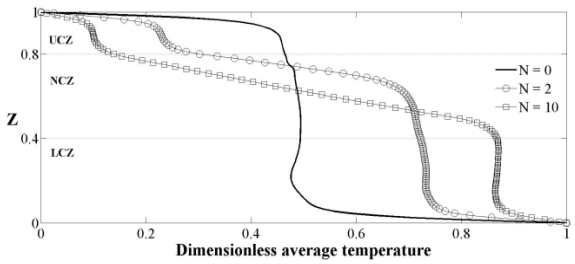

Fig. 18. Effect of buoyancy ratio on the average temperature profile in a salt–gradient pond at $\tau = 0.045$. ($Ra_T = 10^7$, Pr = 6, Sc = 1000 and A = 3)

When the buoyancy ratio increases (Fig. 18), the average temperature increases considerably in the LCZ and has maximum values for N = 10, and its value decreases in the NCZ. In the UCZ, the average temperature decreases because the salt increases the density of the fluid to the pond's bottom. Fig. 18 shows also that the increase of buoyancy ratio will reduce the convective heat transfer in the NCZ.

The effect of buoyancy ratio on the development of the average concentration profile in a salt–gradient pond for $Ra_T = 10^7$ and A = 3 at $\tau = 0.045$ is shown in Fig. 19. It is observed from Fig. 19 that the average concentration profile becomes almost confused with the initial profile in the NCZ for a buoyancy ratio equal to 10. The increase of buoyancy ratio decreases the average concentration in the UCZ and increases the average concentration in the LCZ. The importance buoyancy ratio can be explained by its considerable role in the maintaining of high temperature in the LCZ.

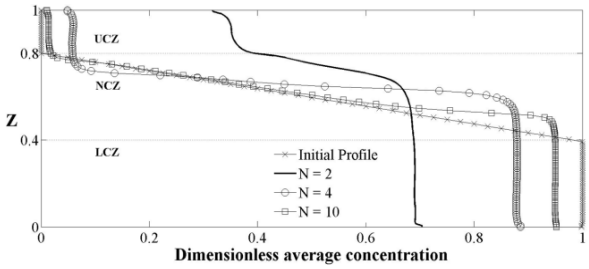

Fig. 19. Effect of buoyancy ratio on the average concentration profile in a salt–gradient pond at $\tau = 0.045$. ($Ra_T = 10^7$, Pr = 6, Sc = 1000 and A = 3)

The effect of thermal Rayleigh number on the development of the average concentration profile in a salt–gradient pond for N = 10 and A = 3 at $\tau = 0.045$ is shown in Fig. 20.

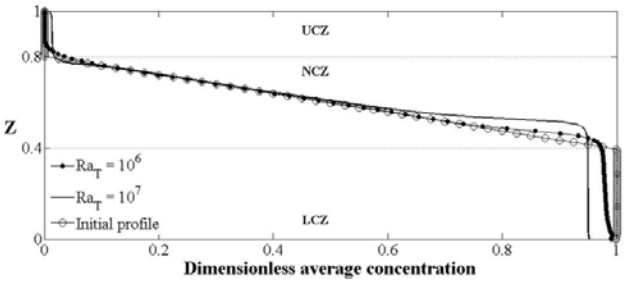

Fig. 20. Effect of Ra_T on the average concentration profile in a salt–gradient pond at $\tau = 0.045$. (N = 10, Pr = 6, Sc = 1000 and A = 3)

Fig. 20 shows that the increase of thermal Rayleigh number will increase the average concentration in the UCZ and will decrease the average concentration in the LCZ. In fact, the increase of temperature in the LCZ causes the diffusion of salt from the bottom to the free surface of the pond. In most of the NCZ, the initial concentration profile is preserved with thermal Rayleigh number.

5. Conclusions

In this work, a two–dimensional numerical study of the effect of thermal Rayleigh number and buoyancy ratio on the fluid flow, heat and mass transfer has been developed to give a fine knowledge of the transient evolution of hydrodynamic, thermal and solute behavior in a salt–gradient pond during the storage of thermal energy. The main conclusions obtained from the present numerical study are given below.

1. Heat transfer by convection is more pronounced at a thermal Rayleigh number equal to 10^6.
2. For a thermal Rayleigh number equal to 10^7, velocity vector fields show the presence of little and large convective cells caused in the UCZ and in the LCZ, respectively.
3. For a buoyancy ratio equal to zero (without salt gradient), it is shown that it is impossible to store thermal energy at the bottom of the convective pond.
4. The increase of buoyancy ratio has a very important effect to store thermal energy in the LCZ and to reduce the convective heat losses across the NCZ. In addition, the stratified fluid layers are stable at high values of buoyancy ratio, which proves an increasing of temperature in the bottom of the pond.
5. It is shown that the value of buoyancy ratio equal to 10 is a limit of salt stratification stability of the salt–gradient pond.

Nomenclature

A	aspect ratio, (=L/H)
C	concentration, (kg/m^3)
ΔC	concentration difference, (kg/m^3)
D	mass diffusivity, (m^2/s)
g	acceleration due to gravity, (m/s^2)
H	height of the cavity, (m)
L	length of the cavity, (m)
Le	Lewis number,
N	buoyancy ratio,
p	pressure, (Pa)
P	dimensionless pressure,
Pr	Prandtl number,
Ra_T	thermal Rayleigh number,
Ra_S	solutal Rayleigh number,
Sc	Schmidt number,
t	time, (s)
T	temperature, (K)
ΔT	temperature difference, (K)
u, w	velocity components, (m/s)
U, W	dimensionless velocity components,
x, z	cartesian coordinates, (m)
X, Z	dimensionless cartesian coordinates,

Greek symbols

α	thermal diffusivity, (m^2/s)
β_T	coefficient of thermal expansion, (K^{-1})
β_S	coefficient of solutal expansion,(m^3/kg)
λ	thermal conductivity, (W/m K)
ν	cinematic viscosity, (m^2/s)
μ	dynamic viscosity, (kg/m s)
ρ	density, (kg/m^3)
φ	dimensionless concentration,
θ	dimensionless temperature,
τ	dimensionless time,

Subscripts

a	ambient,
h	hot,
max	maximum value,
min	minimum value,
l	local,
S	solute.

References

[1] H. Tabor, Solar ponds: large-area collectors for power production, *Solar Energy*, 7 (1963) 189.

[2] S. Shahar, US Patent 337291, 1968.

[3] H.C. Bryant, I. Colbeck, A solar pond for London, *Solar Energy*, 19 (1977) 321.

[4] M.N.A. Hawlader, The influence of the extinction coefficient on the effectiveness of solar ponds, *Solar Energy*, 25 (1980) 461-464.

[5] T.A. Newell, R.G. Cowie, J.M. Upper, M.K. Smith, G.L. Cler, Construction and operation activities at the University of Illinois salt-gradient solar pond, *Solar Energy*, 45 (1990) 231-239.

[6] F.B. Alagao, A. Akbarzadeh, P.W. Johnson, The design, construction and initial operation of a closed-cycle salt-gradient solar pond, *Solar Energy*, 53 (1994) 343-351.

[7] J. Srinivasan, A. Guha, The effect of bottom reflectivity on the performance of a solar pond, *Solar Energy*, 39 (1987) 361-367.

[8] K. Jamal, S. Khashan, Parametric study of a solar pond for Northern Jordan, *Solar Energy*, 21 (1996) 939-946.

[9] K. Huseyin, F.H. Korhan, A. Binark, Solar pond conception-experimental and theoretical studies, *Energy Convers. Manag.*, 41 (2000) 939-951.

[10] L. Huanmin, H.P. Andrew, H.D. Swift, J. Hein, C. John, Advancements in Salinity Gradient Solar Pond Technology Based in Sixteen Years of Operational Experience, *J. Solar Energy Eng.*, 126 (2004) 759-767.

[11] A. Kumar, V.V.N. Kishore, Construction and operational experience of a 6000 m^2 solar pond at Kutch-Indian, *Solar Energy*, 65 (1999) 237-249.

[12] M. Hammami, M. Mseddi, M. Baccar, Transient natural convection in an enclosure with vertical solutal gradients, *Solar Energy*, 81 (2007) 476-487.

[13] R. Boudhiaf, A. Ben Moussa, M. Baccar, A Two-Dimensional Numerical Study of Hydrodynamic, Heat and Mass Transfer and Stability in a Salt Gradient Solar Pond, *Energies*, 5 (2012) 3986-4007.

[14] S.V. Patankar, Numerical heat transfer and fluid flow, Hemisphere Publishing Corporation: Washington, DC, USA, 1980.

Corresponding author' information

Ridha BOUDHIAF, born in Kasserine, Tunisia. He has the Ph. D. degree in Chemical–Process Engineering at the National Engineers School of Gabès (ENIG), University of Gabès, Tunisia, and he is a researcher in the Computational Fluid Dynamics and Transfer Phenomena (CFDTP) at National Engineers School of Sfax (ENIS), University of Sfax, Tunisia. He is also a professor of process engineering in Higher Institute of Technological Studies of Gafsa, University of Gafsa, Tunisia.

Current and previous research interests: Renewable Energy, Energy Storage, Energy Conversion, Fluid Flow, Heat and Mass Transfer, and Numerical Simulation.

The director of the CFDTP is **Mounir BACCAR**. He is a professor in the Mechanical Engineering Department of the National Engineers School of Sfax (ENIS), University of Sfax, Tunisia.